Springer

Journal of
Mechanical
Science and
Technology

Journal of Mechanical Science and Technology 23 (2009) 2357~2365

www.springerlink.com/content/1738-494x
DOI 10.1007/s12206-009-0210-1

Simultaneous measurement of particle and fluid velocities in particle-laden flows †

D. X. Jin[1] and D.-Y. Lee[2,*]

[1]*School of Energy and Power Engineering, Dalian University of Technology, Dalian 116024, China*
[2]*Energy Mechanics Research Center, Korea Institute of Science and Technology, Seoul 136-791, Korea*

(Manuscript Received June 9, 2008; Revised November 17, 2008; Accepted February 11, 2009)

Abstract

For the velocity measurement in a particle-laden fluid flow, the fluid velocity and the inherently dispersed particle velocity can be analyzed by using PIV and PTV, respectively. Since the PIV result statistically represents the average displacement of all the particles in a PIV image, it is inevitable that the PIV result includes the influence of the dispersed particles' displacement if a single CCD camera is used to simultaneously measure the fluid velocity and the dispersed particle velocity. The influence of dispersed particles should be excluded before the PIV analysis in order to evaluate the fluid velocity accurately. In this study, the optimum replacement brightness of dispersed particles to minimize the false influence of dispersed particles on the PIV analysis was theoretically derived. Simulation results show that the modification of dispersed particle brightness can significantly reduce the PIV error caused by the dispersed particles. This modification method was also verified in the analysis of an actual experimental case of the particle-laden fluid flow in a triangular grooved channel.

Keywords: Particle-laden flow; Dispersed particle; PIV; PTV; Simultaneous measurement

1. Introduction

In many cases, the fluid velocity can be measured by using a PIV method [1, 2] and the particle velocity by a PTV method [3-5]. In a particle-laden flow, the PIV tracer particles added to the fluid for PIV investigation should be small enough to be visually distinguishable from the particles inherently dispersed in the fluid. It is recommended that the diameter of the tracer particles be about 0.1 times smaller compared to the inherently dispersed particles [6]. In this respect, hereafter we call the particles inherently dispersed in the fluid as the large particles and the PIV tracer particles as the small particles.

Wereley et al. [6] measured both the particle velocity and the fluid velocity in a rotating filter at a cross-section perpendicular to the rotation shaft using PTV and PIV, respectively. The images for both PTV and PIV analyses were obtained simultaneously with a single CCD camera. The images for PTV analysis were obtained by extracting only the large particles from the native images taken by the CCD camera based on their brightness and sizes. Then, the images with the large particles having been removed leaving only small PIV tracer particles were used for the PIV analysis. In their measurement, the volume concentration of the large particles was limited to a very small value, i.e., around 10^{-4} (m^3 particle/m^3 fluid), which corresponds to an area fraction of only about 0.1-1.0% in the PIV image.

Kiger and Pan [7] introduced a PIV technique for the simultaneous measurement of dilute solid-liquid, two-phase turbulent flows. In the technique, a two-dimensional median filter was employed to filter out small tracer particles' image. Only the large particles were left in the image and their motions were then

† This paper was recommended for publication in revised form by Associate Editor Yang Na

*Corresponding author. Tel.: +82 2 958 5674, Fax.: +82 2 3408 4333
E-mail address: ldy@kist.re.kr

calculated with a correlation tracking algorithm. The image of only tracer particles was obtained by simply subtracting the filtered image from the original image. The velocity field of the fluid was then calculated through a standard cross-correlation method applied to images of the tracer particles. The technique was evaluated as successful for a dilute suspension of the large particles with a small difference in brightness between the large particles and the small tracer particles.

Khalitov and Longmire [8] simultaneously measured solid velocities and gas velocities in a particle-laden gas flow using a single camera. They used a phase discrimination algorithm employing second-order intensity gradients to identify the dispersed solid objects and the tracer objects. The solid velocities were computed by PTV and the gas velocities by PIV. In the gas velocity calculation, the areas of removed solid particles were replaced with a uniform low intensity.

Zhang et al. [9] simultaneously measured the wind velocity and the wind-blown sand velocity by employing the PIV and PTV techniques, respectively. The two-phase particle images were simultaneously captured by a single camera and the wind tracer-only images were obtained by subtracting the sand particle images from the raw images. In order not to delude the subsequent wind velocity calculation via the PIV cross-correlation algorithm, the regions of removed sand particle images were replaced with the local averaged background intensity.

Since the PIV results statistically represent the average displacement of all the particles in a PIV image, it is inevitable that the results include the influence of the large particles' displacement if the large particles appear in the image. Therefore, if the large particle's velocity differs from the fluid velocity, the PIV result cannot correctly represent the fluid displacement. Consequently, when a single camera is used to obtain simultaneous velocities of large particles and fluid in a particle-laden fluid flow, the influence of large particles should be excluded before the PIV analysis in order to evaluate the fluid velocity accurately. This can be accomplished by modifying the image of the large particle to make it more indistinguishable from the background.

In this study, we theoretically derive the optimum replacement brightness of large particles when the original images contain all the small and large particles to minimize the false influence of large particles on the PIV analysis. This modification method can be applied even to a fluid with such a high concentration of large particles that the area fraction of the large particles in the image reaches as high as 30%. For the verification of this method, a process of particulate deposition in a triangular grooved channel is analyzed employing this method.

2. Simultaneous measurement technique

Single exposure/double frame, cross-correlation based PIV is probably the most commonly used method in PIV. This method uses two serial images of tracer particles to calculate relative displacement of the particles, as shown schematically in Figs. 1 and 2. The displacement is evaluated for each sub-image (interrogation window) taken from the PIV image by subdividing it into multiple small images. The interrogation window A_g in the second image is taken larger than the interrogation window A_f in the first image so that it may include all the possible displacements of the particles within A_f. The average spatial displacement of particles can be estimated through a statistical technique of cross-correlation between the interrogation windows A_f and A_g. The

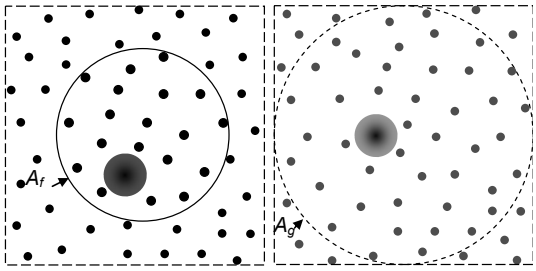

(a) Interrogation window A_f (b) Interrogation window A_g

Fig. 1. Schematics of serial images for PIV analysis of a particle-laden fluid flow.

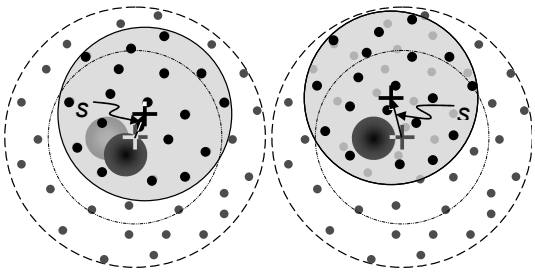

(a) Best match for the fluid (b) Best match for the large particle

Fig. 2. Correlation process between interrogation areas f and g in the PIV calculation.

cross-correlation is given by

$$R(\mathbf{s}) = \int_{A_f} f(\mathbf{x}) g(\mathbf{x}+\mathbf{s}) d\mathbf{x} \tag{1}$$

where f and g are the respective brightness functions of A_f and A_g, and $\mathbf{s}$ is the separation vector between A_f and A_g, as shown in Fig. 2. From a statistical point of view, the separation vector showing the highest correlation peak represents the relative displacement for the best match between the interrogation windows A_f and A_g [10].

If large particles with different velocities from the small PIV particles are included in the interrogation windows, the correlation function will be affected by the large particles. As a result, the determination of the displacement of small PIV particles based on the correlation function is distorted. Fig. 2 is a schematic presentation showing the influence of a large particle on the cross-correlation. It can be expected that there exist two local correlation peaks corresponding to the best matches for the small PIV particles and for the large particle, respectively. Even if the image of a large particle is removed from both interrogation windows by substituting zero brightness to the area occupied by the large particle, the influence of the large particle will not vanish because the correlation still exists between the areas having zero brightness. To reduce the false influence of a large particle on the PIV result, the large particle in the native images must be replaced with a non-zero brightness to minimize distortion of the correlation function caused by the existence of the large particle.

On the other hand, the velocity of each large particle can be obtained from a match probability based two-frame PTV analysis [4, 5]. The images of the large particles for the PTV analysis can be extracted from the native images if the large particles are visually identified based on brightness and size. In this case, the PTV result is hardly affected by the existence of small PIV particles.

2.1 Derivation of optimal brightness value to replace the large particles

Let's first consider the case where only one image out of the two serial CCD images has large particles, while no large particle exists in the other CCD image. If we take the interrogation window A_f as the image having large particles, the cross-correlation can be expressed as

$$\begin{aligned} R_f(\mathbf{s}) = & \int_{A_f - \sum_{i=1}^{n} A_{p,i}} f(\mathbf{x}) g(\mathbf{x}+\mathbf{s}) d\mathbf{x} \\ & + \alpha \int_{\sum_{i=1}^{n} A_{p,i}} g(\mathbf{x}+\mathbf{s}) d\mathbf{x} \end{aligned} \tag{2}$$

where n and $A_{p,i}$ are the number of the large particles and the area occupied by the i^{th} large particle, respectively, and α is the brightness value to replace the large particles. The difference in the correlation between the cases with and without large particles can be given by subtracting Eq. (1) from Eq. (2) as

$$\begin{aligned} \Delta R_f = R_f - R &= \int_{\sum_{i=1}^{n} A_{p,i}} \left[\alpha - f(\mathbf{x})\right] g(\mathbf{x}+\mathbf{s}) d\mathbf{x} \\ &\approx \sum_{i=1}^{n} A_{p,i} \left[\alpha - f(\mathbf{X}_i)\right] g(\mathbf{X}_i + \mathbf{s}) \end{aligned} \tag{3}$$

where $\mathbf{X}_i$ is the position vector to the center of the i^{th} large particle. In the simplification of the above equation, the area occupied by each large particle is presumed to be relatively small compared to the interrogation area, A_f.

Eq. (3) implies the distortion of the correlation function due to the existence of the large particles. To minimize the correlation difference for any positions of the large particles and any fluid displacement, the replacement brightness should satisfy the following condition:

$$\frac{d}{d\alpha} \int_{A_f} d\mathbf{X}_1 \cdots \int_{A_f} d\mathbf{X}_n \int_{A_s} \Delta R_f^2 d\mathbf{s} = 0 \tag{4}$$

where A_s is the domain of the separation vector, which includes the largest possible relative displacement between A_f and A_g.

Substituting Eq. (3) into the left hand side of Eq. (4) yields

$$\begin{aligned} & \frac{d}{d\alpha} \int_{A_f} d\mathbf{X}_1 \cdots \int_{A_f} d\mathbf{X}_n \int_{A_s} \Delta R_f^2 d\mathbf{s} = \\ & 2 \int_{A_f} \sum_{i=1}^{n} A_{p,i} \left[\alpha - f(\mathbf{X}_i)\right] G_i d\mathbf{X}_i \end{aligned} \tag{5}$$

where G_i is the abbreviated expression of the following:

$$\begin{aligned} G_i &= \int_{A_f} d\mathbf{X}_1 \cdots \int_{A_f} d\mathbf{X}_{i-1} \int_{A_f} d\mathbf{X}_{i+1} \\ &\quad \cdots \int_{A_f} d\mathbf{X}_n \int_{A_s} \sum_{j=1}^{n} A_{p,j} g(\mathbf{X}_i + \mathbf{s}) g(\mathbf{X}_j + \mathbf{s}) d\mathbf{s} \\ &= A_f^{n-2} \sum_{\substack{j=1 \\ j \neq i}}^{n} A_{p,j} \int_{A_f} d\mathbf{X}_j \int_{A_s} g(\mathbf{X}_i + \mathbf{s}) g(\mathbf{X}_j + \mathbf{s}) d\mathbf{s} \\ &\quad + A_f^{n-1} A_{p,i} \int_{A_s} g^2(\mathbf{X}_i + \mathbf{s}) d\mathbf{s} \end{aligned} \tag{6}$$

In PIV analysis, the tracer particles should appear evenly distributed over the image; otherwise the location of the correlation peak is not dependent only on the velocity field, but is biased depending on the distribution of the tracer particles [2]. Therefore, in general, the brightness is distributed homogeneously in PIV images. In such cases, the following relation is satisfied regardless of the location of the large particle, X.

$$\frac{1}{A_s} \int_{A_s} g^2(\mathbf{X} + \mathbf{s}) d\mathbf{s} \approx const \equiv \langle g^2 \rangle \tag{7}$$

$$\frac{1}{A_s} \int_{A_s} g(\mathbf{X} + \mathbf{s}) d\mathbf{s} \approx const \equiv \langle g \rangle \tag{8}$$

Substituting Eqs. (7) and (8) into Eq. (6) we get

$$\begin{aligned} G_i &\approx A_f^{n-1} \langle g \rangle \sum_{\substack{j=1 \\ j \neq i}}^{n} A_{p,j} \int_{A_s} g(\mathbf{X}_i + \mathbf{s}) d\mathbf{s} + A_f^{n-1} A_{p,i} A_s \langle g^2 \rangle \\ &\approx A_f^{n-1} A_s \left(\langle g \rangle^2 \sum_{\substack{j=1 \\ j \neq i}}^{n} A_{p,j} + A_{p,i} \langle g^2 \rangle \right) = const > 0 \end{aligned} \tag{9}$$

Substituting Eq. (9) into Eq. (5), and then the result into the left hand side of Eq. (4) yields

$$\left(\sum_{i=1}^{n} A_{p,i} G_i \right) \int_{A_f} \left[\alpha - f(\mathbf{X}_i) \right] d\mathbf{X}_i = 0 \tag{10}$$

To satisfy Eq. (10), the optimum brightness, α, to replace the particles is found by

$$\alpha = \frac{1}{A_f} \int_{A_f} f(\mathbf{X}) d\mathbf{X} = \langle f \rangle \tag{11}$$

This result implies that when only one CCD image has large particles while there is no large particle in the other CCD image, the optimum brightness to replace the large particles in the interrogation window is the average brightness of the background image, including small PIV tracer particles.

Now, let's consider the case where large particles exist in both serial CCD images. If we neglect the effect of overlap between the large particles in interrogation window A_f and those in interrogation window A_g, the correlation difference is given by:

$$\Delta R = \Delta R_f + \Delta R_g \tag{12}$$

where ΔR_g is the correlation difference when the large particles exist only in interrogation window A_g.

Since ΔR_f and ΔR_g are independent of each other, the minimization of ΔR is equivalent to the minimization of ΔR_f and ΔR_g individually. Therefore, even when both the serial CCD images have large particles, the optimum replacement value for the large particles is again the mean brightness of the background image, including small PIV tracer particles.

As mentioned in the previous section, the displacement of the large particle affects the correlation function and thus the PIV result. To prevent this effect, it is required to make the large particle more difficult to find its corresponding pair from the correlating image. This can be accomplished by modifying the image of the large particle to make it more indistinguishable from the background image. From a statistical point of view, the best modification of the large particle is to replace the large particle with the average brightness of the background image, as shown previously in this section.

2.2 Verification of the algorithm

The modification method for large particle brightness was first tested with artificially generated particle images. The images were generated by adding the images of large particles to the standard PIV images with a known velocity field [11]. The interrogation window was set at 32×32 pixels and 50% overlap was

permitted. The randomly distributed large particles were square with a uniform size of 7×7 pixels. The area occupied by the large particles is 20% of the interrogation window, if not otherwise mentioned. Fig. 3(a) shows one of the artificial images used for the verification test. The large square white spots represent the large particles. The background images with the small particles were adopted from the work of Okamoto et al. [11]. The given fluid velocity field is shown in Fig. 3(b). The maximum fluid displacement was 6.2 pixels. The large particles were given a uniform displacement. The displacement of the large particles was obtained from the PTV and was found consistent with the given value (Fig. 3(c)).

The effects of the replacement value on the PIV analysis are shown in Figs. 3(e)-(h). When the images of large particles are replaced by the average brightness of the interrogation window, the PIV analysis on the modified images yields a result very close to the given velocity field, as shown in Figs. 3(e) and (f).

Meanwhile, if the images of large particles are removed and replaced by zero brightness, the PIV analysis results in a significant error, as shown in Figs. 3(g) and (h). In this case, the error vectors shown in Fig. 3(h) are classified as either very large or very small. The very large error vectors are found to be nearly the same as the velocity differences between the large particles and the fluid shown in Fig. 3(d). This implies that the fluid displacements were calculated as the displacements of the large particles instead of that of the fluid.

To explain the reason for the two-state characteristics of the PIV error, the distribution of the correlation function is shown schematically in Fig. 4, in the case of substituting zero brightness for a large particle. In this figure, s is the degree of the separation, l_p the size of the large particle, d_r the relative displacement of the large particle to the fluid, and R_0 is the background value when interrogation windows A_f and A_g are not correlated at all. For the sake of simplicity, the displacement of the fluid is assumed to be zero in this case, such that there exists a local maximum of the correlation function at s=0.

Since the image of the large particle is substituted by zero brightness, the area correlated with the large particle of zero brightness does not contribute to the correlation (see Eq. (2)), causing a decrease in the correlation value. The decrease in the correlation value becomes the minimum when the large particle is completely overlapped with that in the other inter-

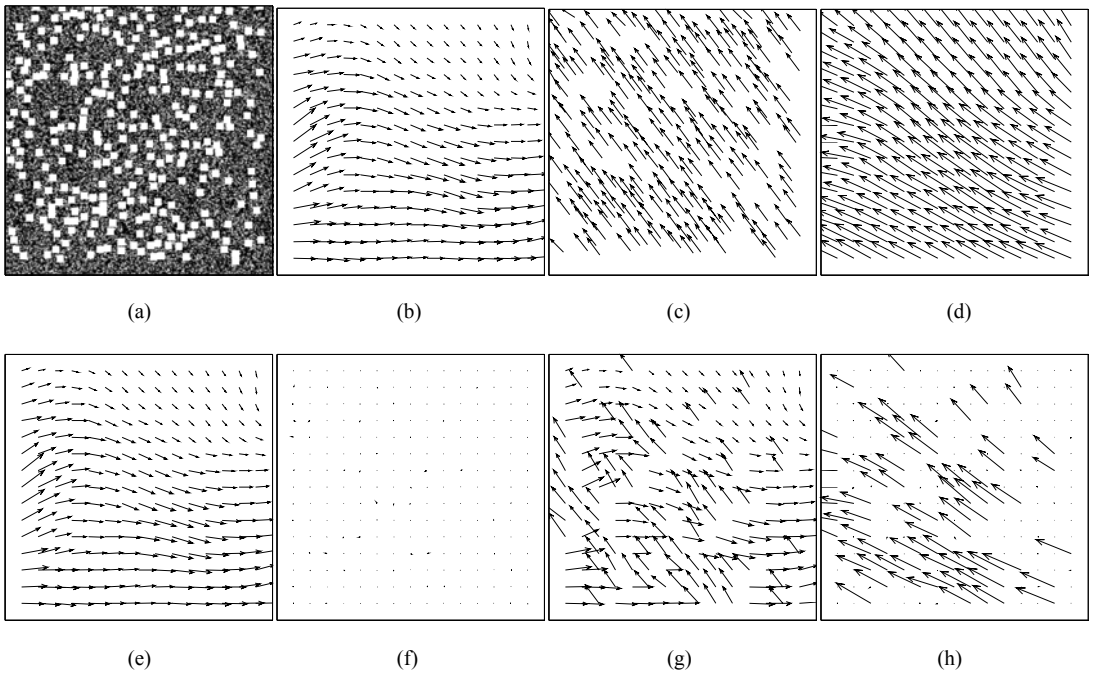

Fig. 3. Simulation results of PIV and PTV simultaneous measurement: (a) PIV+PTV image, (b) given fluid velocity field, (c) PTV result, (d) velocity difference between the large particles and fluid, (e) PIV result when $\alpha = \langle f \rangle$ and $\beta = \langle g \rangle$, (f) PIV error when $\alpha = \langle f \rangle$ and $\beta = \langle g \rangle$, (g) PIV result when $\alpha = 0$ and $\beta = 0$, (h) PIV error when $\alpha = 0$ and $\beta = 0$.

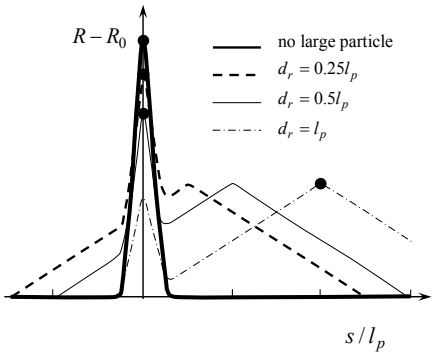

Fig. 4. Correlations for various relative displacements between the large particles and fluid when $\alpha = 0$ and $\beta = 0$.

rogation window, as can be inferred from Fig. 2. As a result, another local maximum in the correlation function occurs at the separation corresponding to the displacement of the large particle.

As shown in Fig. 4, if the relative displacement between the large particle and the fluid is small, the highest correlation peak occurs at the separation corresponding to the fluid displacement regardless of the relative displacement of the large particle. This is because the decrease in the local maximum value of the correlation corresponding to the fluid displacement is not very large, since most of the large particle overlaps with itself and the decrease in the correlation value is not very large. However, as the relative displacement between the large particle and the fluid increases, the correlation value corresponding to the fluid displacement becomes smaller and eventually smaller than the correlation value corresponding to the displacement of the large particle. At that instant, the separation for the highest correlation moves suddenly from the value corresponding to the displacement of the fluid to the value corresponding to the displacement of the large particle. This is the reason for the abrupt change and the two-state characteristics of the PIV error shown in Fig. 3(g).

Fig. 5 displays the effect of the brightness value to replace the large particle on the average error in PIV calculation. The average error was defined as

$$E_{ave} = \frac{1}{N}\sum_{i=1}^{N}\frac{|\mathbf{d}_i - \mathbf{d}_{ei}|}{d_e} \quad , \quad d_e = \frac{1}{N}\sum_{i=1}^{N}|\mathbf{d}_{ei}| \qquad (13)$$

where N is the number of interrogation windows, $\mathbf{d}_i$ and $\mathbf{d}_{ei}$ are the calculated and the exact displacement vectors of i^{th} interrogation window, and d_e is the

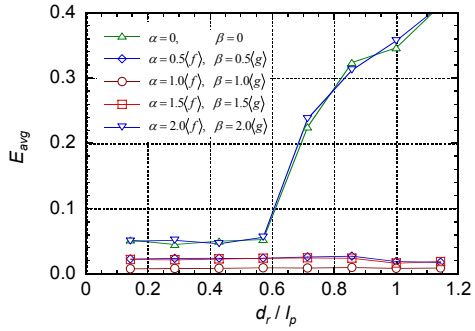

Fig. 5. Variation of the average PIV error with respect to the replacement brightness.

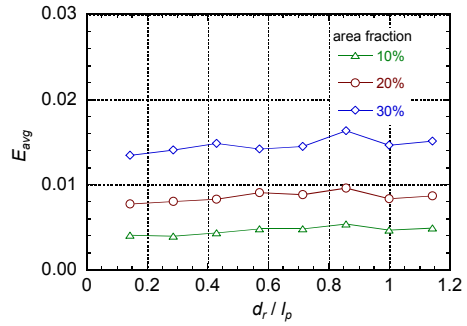

Fig. 6. Variation of the average PIV error with respect to the area fraction of large particles when $\alpha = \langle f \rangle$ and $\beta = \langle g \rangle$.

average magnitude of $\mathbf{d}_{ei}$'s. The abscissa of Fig. 5 represents the average relative displacement between the large particles and the fluid, which was defined as

$$d_r/l_p = \frac{1}{N}\sum_{i=1}^{N}\left|\mathbf{d}_p - \mathbf{d}_{ei}\right|/l_p \qquad (14)$$

Fig. 5 shows that substituting the average brightness for the large particles minimizes the average PIV error caused by the velocity difference between the large particles and the fluid. The larger the brightness difference between the large particles' and the small particles' image, the larger the average PIV error. When the substitution brightness value for the large particles is twice as large as that of the background, the average PIV error suddenly increases around d_r/l_p =0.6. This implies that the separation of the images for the global maximum of the correlation changed from the fluid displacement to the displacement of large particles in many interrogation sub-windows.

Fig. 6 shows the effect of the area density of the large particles when the average brightness of the

background image was substituted for the large particles. Though the average PIV error is found to increase with an increase in the area density, the error is smaller than 2% even when the large particles occupy as much as 30% of the entire image.

3. Application to a grooved channel flow

For the verification of the modification method, a simultaneous velocity measurement of the fluid and the dispersed particles has been performed for a particle-laden fluid flow in a triangular grooved channel. This type of flow situation can be found in compact heat exchangers dealing with dirty fluids. In such cases, the information on the simultaneous velocities of the fluid and the particles is very important to investigate the interaction between the fluid and the particles.

The experimental setup is the same as that of Jin et al. [12]. Fig. 7 shows the triangular grooved channel having a height (H) of l5 mm, a length (L) of 18 mm and a depth (a) of 9 mm. The channel is composed of 30 grooves arranged in the flow direction and is 187.5 mm wide.

The schematic diagram of the experimental setup is shown in Fig. 8. To obtain a uniform velocity at the entrance of the grooved channel, a bell-mouth-type channel entrance was designed. Pyrex glass and acrylic plate were applied to both sides of the channel and to the bottom of the channel, respectively, for the internal visualization of the flow. The PIV system used in this study consists of a laser, a 480 by 420

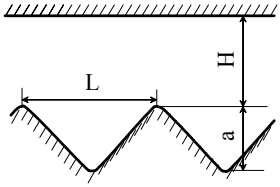

Fig. 7. Grooved channel.

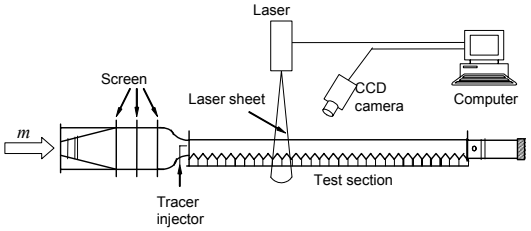

Fig. 8. Schematic diagram of the experimental setup.

resolution CCD camera and a computer which controls the PIV system. The PIV tracer was polystyrene particles having a mean diameter of 25 μm and the PTV particles were also polystyrene particles with a diameter range of 200-300 μm. The specific gravity of the polystyrene particle was 1.04. The experiment was performed at the condition of steady flow with the Reynolds number of 370. The Reynolds number was based on the channel height and the flow velocity at the smallest cross section of the channel.

The larger particles were detected based on the brightness and size of the particles in the CCD image by using the dynamic threshold-binarization method [5]. The velocity of the individual large particle was obtained by PTV. The images for the PIV analysis of the fluid velocity were prepared by replacing the large particles with the average brightness of the image from which the large particles were removed.

Fig. 9 shows the flow visualization and the results of the simultaneous measurement. The flow visualization was obtained by overlapping 20 successive CCD images taken at time intervals of 3/25 s. The PIV results show that a vortex rotates slowly inside the groove and the main stream outside the groove is hardly affected by the recirculating flow within the groove. Contrary to the fluid, the large particles in the main stream move downward to enter the groove valley and gradually slow to deposit onto the groove surface. The velocities of the large particles in the PTV result are very similar to the behavior of large particles recognized from the flow visualization results. The fluid velocity measurement is found to be almost unaffected by the existence of the large particles.

The effect of the substitution brightness for the large particles is shown in Fig. 10. In this figure, the definition of the average PIV error in Eq. (13) is slightly modified, since the exact fluid velocity is not known in this experimental case. The modified definition is

$$E_{ave} = \frac{1}{N}\sum_{i=1}^{N}\frac{|\mathbf{d}_i - \mathbf{d}_{0i}|}{d_0} \quad , \quad d_0 = \frac{1}{N}\sum_{i=1}^{N}|\mathbf{d}_{0i}| \qquad (15)$$

where $\mathbf{d}_{0i}$ is the calculated displacement vector of i^{th} interrogation window with the replacement value of the average brightness.

Fig. 10 shows the average error depends largely on the replacement brightness and increases up to more

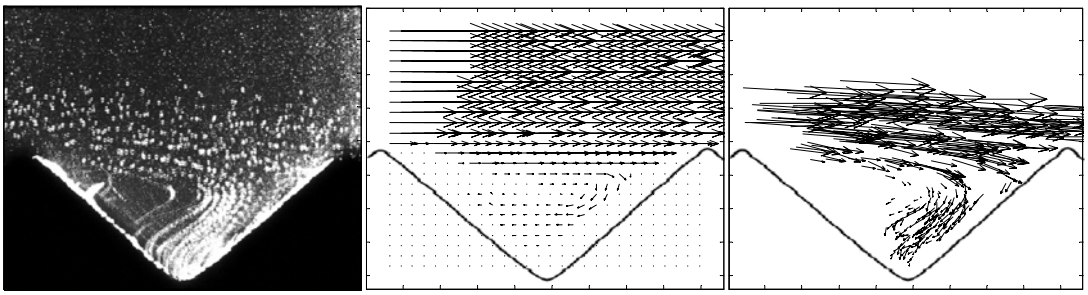

(a) Flow visualization (b) PIV result (c) PTV result

Fig. 9. Experimental results of simultaneous measurement.

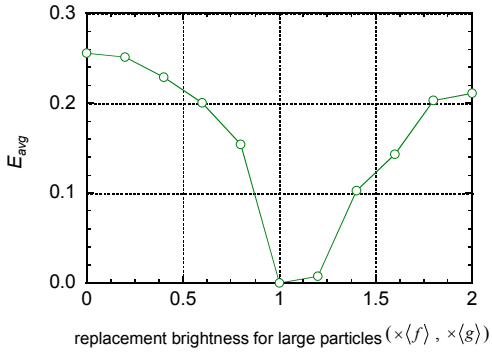

Fig. 10. Effect of replacement brightness for large particles on PIV calculation.

than 20% when the replacement brightness value is smaller or larger than the average brightness of the image.

4. Conclusions

A method to minimize the false influence of large particles on the PIV analysis is theoretically derived in this study. In this method, the velocities of the fluid and the dispersed particles are analyzed by PIV and PTV, respectively, from the same flow images taken by a single CCD camera. For PIV measurement, the fluid is added with tracer particles smaller than the particles inherently dispersed in the fluid so that they can be distinguishable in the CCD image. In this case, as a PIV result represents the average displacement of all the particles in an interrogation window, it will include an error caused by the relative displacement of the inherently dispersed particles to those of the tracer particles. To reduce the false influence of the inherently dispersed particles in the PIV calculation, the image is required to be modified so that the particles are less distinguishable from the background images. To this end, it is analyzed in this study that the optimal replacement value for the large particles in the PIV analysis is the average brightness of the background image. The simulation results show that the modification method can significantly reduce the PIV error caused by the large particles. This method is found to be applicable even to a fluid with such a high concentration of large particles that the area fraction of the large particles in the image reaches as high as 30%.

This method was also verified in the analysis of an actual case of the particle-laden fluid flow in a triangular grooved channel. In this case, the large particles flowing into the groove slow gradually and eventually deposit on the groove surface, while the fluid in the groove rotates to form a steady vortex. Regardless of the velocity difference between the particles and the fluid, the fluid velocity can be measured correctly by this method.

Nomenclature

a : Groove depth (m)
A : Area [pixel^2] or interrogation window
$\mathbf{d}$: Displacement vector (pixel)
d : Displacement (pixel)
E_{avg} : Average value of the PIV evaluation error
f : Brightness function of the first interrogation window
g : Brightness function of the second interrogation window
H : Channel height (m)
l_p : Characteristic length of the large particle [pixel]
L : Groove length (m)
n : Number of large particles
N : Number of interrogation windows
R : Correlation function

s : Separation vector [pixel]
X : Position vector [pixel]

Greek

A : Optimal replacement value for the large particle in the interrogation window f
B : Optimal replacement value for the large particle in the interrogation window g
r : Relative

Subscripts

e : Exact
f : Interrogation window A_f
g : Interrogation window A_g
p : Particle

References

[1] R. J. Adrian, Particle-imaging techniques for experimental fluid mechanics, *Ann. Rev. Fluid Mech.*, 23 (1991) 261-304.
[2] J. Westerweel, Fundamentals of digital particle image velocimetry, *Meas. Sci. Technol*., 8 (1997) 1379-1392.
[3] Y. G. Guezennec, R. S. Brodkey, N. Trigui and J. C. Kent, Algorithm for fully automated three-dimensional particle tracking velocimetry, *Exp. Fluids*, 17 (1994) 209-219.
[4] S. J. Baek and S. J. Lee, A new two-frame particle tracking algorithm using match probability, *Exp. Fluids*, 22 (1996) 23-32.
[5] K. Ohmi and H. Y. Li, Particle-tracking velocimetry with new algorithms, *Meas. Sci. Technol*., 11 (2000) 603-616.
[6] S. T. Wereley, A. Akonur and R. M. Lueptow, Particle-fluid velocities and fouling in rotating filtration of a suspension, *J. Membrane Sci*., 209 (2002) 469-484.
[7] K. T. Kiger and C. Pan, PIV technique for the simultaneous measurement of dilute two-phase flows, *J. Fluids Eng*., 122 (2000) 811-818.
[8] D. A. Khalitov and E. K. Longmire, Simultaneous two-phase PIV by two-parameter phase discrimination, *Exp. Fluids*, 32 (2) (2002) 252-268.
[9] W. Zhang, Y. Wang and S. J. Lee, Simultaneous PIV and PTV measurements of wind and sand particle velocities, *Exp. Fluids*, (2008) DOI: 10.1007/s00348-008-0474-8.
[10] R. C. Gonzalez and R. E. Woods, *Digital Image Processing*, 2nd ed., New Jersey: Prentice-Hall, (2002).
[11] K. Okamoto, S. Nishio, T. Saga and T. Kobayashi, Standard images for particle-image velocimetry. *Meas. Sci. Technol*., 11 (2000) 685-691.
[12] D. X. Jin, Y. P. Lee and D.-Y. Lee, Effects of the pulsating flow agitation on the heat transfer in a triangular grooved channel, *Int. J. Heat Mass Transfer*, 50 (2007) 3062-3071.

Dong-Xu Jin received his B.S. and M.S. degrees in Thermal Engineering from Beihang University in 1992 and 1995, respectively. He then received his Ph.D. degree from Pohang University of Science and Technology, Korea, in 2003. Dr. Jin is currently a professor at the School of Energy and Power Engineering at Dalian University of Technology in Dalian, China. His research interests include heat transfer enhancement, two-phase flow, and heat pump and refrigeration systems.

Dae-Young Lee received his B.S., M.S. and Ph.D degrees from Seoul National University in 1987, 1989, and 1994, respectively. Dr. Lee is currently a Principal Research Scientist of the Korea Institute of Science and Technology in Seoul, Korea. His research interests cover the heat and mass transfer enhancement by the oscillatory flow excitation, the heat and mass transfer in porous media, and the thermally activated air conditioning technologies.